Attempts were made to prepare copper niobium oxyfluorides with varying amounts of fluorine. The two procedures in the fluorination of $CuNb_2O_6$ involved either the use of H_2/Ar as the carrier gas or the use of pure hydrogen. The former method gave essentially identical products between 600 and 800 °C. Fluorination did not occur below 600 °C. The latter procedure tended to result in the formation of decomposition products.

In view of these observations, it can be concluded that the limit of fluorination was reached and that the maximum amount of fluorination achieved corresponded to the compound $CuNb_2O_{5.3}F_{0.7}$. Moreover, the high electrical conductivity of this compound may be attributed to some delocalization of the 3d electrons probably via metal–oxygen–metal overlap. It is of interest to note that such delocalization occurs despite the presence of fluoride ions which favor localization of 3d electrons.

Acknowledgment. The authors acknowledge the National Science Foundation, Washington, D.C., Contract No. DMR-77-11396, for the support of Bijan Khazai. Acknowledgment is also made to the Office of Naval Research, Arlington, Va., for the support of Kirby Dwight. In addition, the authors acknowledge the support of the Materials Research Laboratory Program at Brown University.

Registry No. $CuNb_2O_6$, 12273-00-6; $CuNb_2O_{5.3}F_{0.7}$, 73197-82-7.

Contribution from the Department of Chemistry,
Clarkson College of Technology, Potsdam, New York 13676

Synthesis of Copper Thioxo- and Dithioimidodiphosphinates. Infrared and Raman Spectra of Imidodiphosphinates

O. SIIMAN* and J. VETUSKEY

Received August 22, 1979

Syntheses of several tetraphenyldithioimidodiphosphinate (L) copper complexes, $[Cu^{I}_4L_3^+][Cu^{I}Cl_2]CCl_4$, $[Cu^{I}_4L_3^+][ClO_4^-]$, $Cu^{I}_3L_3$, $Cu^{I}_3L_3 \cdot 2^1/_2CCl_4$, Cu_3L_4, and $[Cu^{II}(NH_3)_4^{2+}][L^-]_2$, and tetraphenylthioxoimidodiphosphinate (L′) complexes, $Cu^{II}L'_2$ and $Ni^{II}L'_2$, are described. Electronic absorption and EPR spectra of $Cu^{II}L'_2$ and electronic spectra of $Ni^{II}L'_2$ indicated a square-planar MO_2S_2 core geometry for these chelates. Oxidation of L-containing cuprous complexes and redox activity of Cu(II)–L combinations yielded the oxidized ligand, HL′. Infrared and Raman spectra of the above copper chelates as well as HL, NaL, $Mn^{II}L_2$, $Fe^{II}L_2$, and $Co^{II}L_2$ were measured between 1700 and 200 cm^{-1}. The resonance Raman spectrum of $Cu^{II}L_2$ was obtained and compared with similar spectra of Cu_3L_4. The infrared spectra of tetramethyldithioimidodiphosphinates (L″), HL″ and $Co^{II}L''_2$, and the Raman spectrum of HL″ were also measured. Vibrational mode assignments of ν(PN), ν(PO), ν(PC), and ν(MS) and phenyl and methyl group bands are made. Structural and bonding changes are correlated with these vibrational frequencies.

Introduction

Ligands that are identified by the generic name imidodiphosphinate, $(R_2XPNPYR_2)^-$, where R = CH_3 or C_6H_5 and X,Y = S, O, or NH, were first synthesized by Schmidpeter et al.[1] Structure and bonding in dithioimidodiphosphinate (L) ligands make them unique among sulfur donors in several respects: (1) stereochemical trends in $M^{II}L_2$ complexes, M = first-row transition metal; (2) redox behavior of metal and ligand in complex formation; and (3) nonrigidity of chelate ring geometry.

The tetrahedral geometry about P atoms of L was expected to produce appropriate puckering of six-membered chelate rings in $M^{II}L_2$ complexes and so, possibly, induce tetrahedral geometry about the central metal atom. Tetrahedral $M^{II}S_4$ core structures[2] were verified for Mn(II), Fe(II), Co(II), and, surprisingly, Ni(II) and Cu(II) as well. The latter two metal ions generally form square-planar complexes[3] with sulfur ligands. Analyses of d–d bands in the electronic spectra[2a,d] of $M^{II}L_2$ compounds did not indicate an unusually low ligand field strength for this ligand. Nor did magnetic and electronic spectral evidence for planar Ni(II) and Cu(II) complexes[2a,4] with imidodiphosphinates, X = O, Y = O, and X = NH, Y = NH, show that tetrahedral geometry was a common characteristic for all imidodiphosphinates. Since explanations for the observed trend for dithioimidodiphosphinates have not been put forward, we explored the tendency of analogous $M^{II}S_2O_2$ core complexes to form similar tetrahedral structures.

Metal ion–dithioimidodiphosphinate solution redox properties also deviate from the norm for sulfur donor ligands. Stable $Mn^{II}L_2$, $Fe^{II}L_2$, and $Co^{II}L_2$ compounds were isolated[2] in aqueous solution and were immune to the usual air O_2-mediated oxidation of metal and/or ligand. On the other hand, cupric ion–L^- solutions were unstable.[2] Reduction of Cu(II) to Cu(I) and subsequent formation of cuprous complexes under ambient conditions were consistent with a characteristic feature of cupric ion–sulfur ligand systems. Preliminary reports[5] of multinuclear complexes of L with Cu(I) indicated no formation of dimeric disulfides[6] or thioethers[7] that were observed in the oxidation of some thiolate ligands. Details of the syntheses

(1) (a) A. Schmidpeter and H. Groeger, *Z. Anorg. Allg. Chem.*, **345**, 106 (1966); (b) A. Schmidpeter and H. Groeger, *Chem. Ber.*, **100**, 3979 (1967); (c) A. Schmidpeter and J. Ebeling, *ibid.*, **101**, 815 (1968).
(2) (a) A. Davison and E. S. Switkes, *Inorg. Chem.*, **10**, 837 (1971); (b) M. R. Churchill, J. Cooke, J. P. Fennessey, and J. Wormald, *ibid.*, **10**, 1031 (1971); (c) M. R. Churchill and J. Wormald, *ibid.*, **10**, 1778 (1971); (d) O. Siiman and H. B. Gray, *ibid.*, **13**, 1185 (1974); (e) R. D. Bereman, F. T. Wang, J. Najdzionek, and D. M. Braitsch, *J. Am. Chem. Soc.*, **98**, 7266 (1976).
(3) R. H. Holm and M. J. O'Connor, *Prog. Inorg. Chem.*, **14**, 214 (1971).
(4) H. J. Keller and A. Schmidpeter, *Z. Naturforsch., B*, **22**, 231 (1967).
(5) (a) O. Siiman, C. P. Huber, and M. L. Post, *Inorg. Chim. Acta*, **25**, L11 (1977); (b) C. P. Huber, M. L. Post, and O. Siiman, *Acta Crystallogr., Sect. B*, **34**, 2629 (1978).
(6) (a) P. J. M. W. L. Birker and H. C. Freeman, *J. Am. Chem. Soc.*, **99**, 6890 (1977); (b) W. Kuchen and H. Mayatepek, *Chem. Ber.*, **101**, 3454 (1968); (c) S. H. H. Chaston, S. E. Livingstone, T. N. Lockyer, V. A. Pickles, and J. S. Shannon, *Aust. J. Chem.*, **18**, 673 (1965).
(7) (a) K. Olsson and S.-O. Almquist, *Ark. Kemi*, **27**, 571 (1967); (b) A. Fredga and A. Brändström, *ibid.*, **1**, 197 (1950); (c) A. Brändström, *ibid.*, **3**, 41 (1951); (d) J. J. Daly, *J. Chem. Soc.*, 4065 (1964).

0020-1669/80/1319-1672$01.00/0 © 1980 American Chemical Society

and characterization are reported herein.

Chelate ring, MS_2P_2N, structure has been observed to be unusually flexible. X-ray analyses showed that several nonplanar chelate ring configurations (the twisted boat with S,P ends and C_2 axis of symmetry through M,N; the boat with M,N ends and a mirror plane through M,N) were present in $Fe^{II}L_2$[2c] and $Ni^{II}L_2$,[2b] R = CH_3, and that both chelate rings in $Mn^{II}L_2$,[2d] R = C_6H_5, had the twisted boat configuration. Fast time scale fluorescence measurements[8] on $Mn^{II}L_2$ showed a very large Stokes shift in the emission maximum (14 347 cm^{-1}) compared to the first absorption maximum at 18 520 cm^{-1}. The relatively large energy dissipation, much of it undoubtedly into vibrational degrees of freedom, was attributed to a large degree of flexibility in the sulfur donor atom environment. X-ray analysis[5] of $Cu^{I}_4L_3^+$, R = C_6H_5, shows that very nearly planar CuS_2P_2N chelate rings are formed. Therefore, the extent of aromaticity within imidodiphosphinate chelate rings and the effect thereon of S for O substitution are probed.

Vibrational spectroscopy offers an excellent method for examining the above structure–bonding relationships in imidodiphosphinates. Since few details of the vibrational spectra (save some ligand infrared spectra[1a]) of imidodiphosphinate metal complexes have been reported to date, we present a detailed analysis of the infrared, Raman, and, where applicable, resonance Raman spectra of three types of imidodiphosphinates: (1) R = C_6H_5; X, Y = S; (2) R = CH_3; X, Y = S; and (3) R = C_6H_5; X = S; Y = O. Interpretations of spectra are used to draw conclusions about structure and bonding in the complexes.

Experimental Section

Preparation of Compounds. Tetraphenyldithioimidodiphosphinic acid, HL, prepared by the method of Schmidpeter et al.,[1a] was converted to the sodium salt, NaL, by reaction with Na in absolute ethanol, and recrystallized from 1:1 absolute ethanol–anhydrous ethyl ether solution. NaL (0.01 mol) in 100 mL of water was added dropwise to a solution of 0.005 mol of $CuCl_2$ in water. The dark purple precipitate that formed was filtered and dried in vacuo. The crude product, 4.4 g, was dissolved in 50 mL of toluene and chromatographed on a Bio-beads SX-2 (Bio-Rad) column (4 cm × 60 cm) equilibrated with toluene. Three components were separated. The first fraction was purple and contained the bulk of the material. Precipitation with petroleum ether (bp 20–40 °C) and drying under vacuo showed a compound, I, with composition Cu_3L_4. The second fraction was colorless. Evaporation of toluene gave crystals with mp 168–173 °C, that were identified by infrared spectra as the oxidized ligand, HL′, $HOP(C_6H_5)_2NP(C_6H_5)_2S$. The third fraction was yellow and identified as elemental sulfur.

Attempts to recrystallize I from either carbon tetrachloride or dichloromethane led to rapid decomposition with the resulting loss of the purple color. Workup of 5 g of I in 200 mL of hot CH_2Cl_2–CCl_4 solution gave on cooling a pink crystalline product, II, $[Cu^{I}_4L_3^+][Cu^{I}Cl_2^-]CCl_4$. Also, 0.002 mol of $Cu(ClO_4)_2$ in 10 mL of dimethylformamide was added dropwise to 0.001 mol of I in 10 mL of toluene. The white precipitate that formed was filtered and dried in vacuo and identified as $[Cu^{I}_4L_3^+][ClO_4^-]$, III. Recrystallization was performed from 1:1 chloroform–benzene solutions.

Dissolution of I, 0.001 mol, in 50 mL of hot CCl_4 caused loss of purple color and precipitation of colorless crystals of $Cu^{I}_3L_3 \cdot 2^1/_2CCl_4$, IV. Slow elution (>1 h) of I in toluene on the Bio-beads SX-2 column gave an additional fraction after the initial purple one but before that of HL′. Colorless crystals of $Cu^{I}_3L_3$, V, formed upon slow evaporation of toluene.

V was reoxidized temporarily when $Cu(ClO_4)_2$ in dimethylformamide was added dropwise to a toluene solution of V. An intense purple solution formed initially after each addition of $Cu(ClO_4)_2$, but the purple color slowly faded to give a colorless solution. Crystals of $[Cu^{I}_4L_3^+][ClO_4^-]$ separated out after several hours of standing. In another trial V in toluene was mixed with NaL in DMF, and a few drops of hydrogen peroxide (30%) were added. A purple color was observed on adding H_2O_2; a 1:1 ratio of Cu_3L_3:NaL gives a limiting maximum absorbance at 585 nm.

The oxidized ligand, HL′, prepared by a previously described method,[1b] was converted to its sodium salt, NaL′, by dissolution in Na in absolute ethanol and precipitation with anhydrous ether. After recrystallization of NaL′ from ethanol–ether solutions, 0.01 mol of NaL′ in 100 mL of water was added dropwise to 0.005 mol of $CuCl_2$ in water. The brown precipitate was collected and dried in vacuo. Recrystallization from 1:1 chloroform–ether solution gave brown crystals of CuL'_2, VI.

When both 0.01 mol of NaL in water and 0.005 mol of $CuCl_2$ in water were saturated with ammonia gas prior to mixing, the precipitate that formed upon mixing was light blue and upon collection as a solid, VII, was stable only in an NH_3(g) atmosphere. Since loss of NH_3 from VII in vacuo gave the dark violet compound, CuL_2 (VIII), VII was formulated as $[Cu(NH_3)_4^{2+}][L^-]_2$.

Tetramethyldithioimidodiphosphinic acid, HL″, was prepared by published procedures[1c] and converted to its sodium salt, NaL″, by the same route as NaL. NaL″ (0.01 mol) in 100 of mL water was added to 0.005 mol of $CoCl_2$ in water. The dark blue precipitate was collected, washed with water, and dried in vacuo. Recrystallization from 1:5 dichloromethane–hexane solutions gave crystals of $Co^{II}L''_2$.

Elemental Analyses. Imidotetraphenyldithiodiphosphinic acid appeared as colorless crystals, mp 213–214 °C. Anal. Calcd for $C_{24}H_{21}NS_2P_2$: C, 64.13; H, 4.71; N, 3.12. Found: C, 64.05; H, 4.68; N, 3.42.

(Imidotetraphenyldithiodiphosphinato-*S*,*S*′)sodium(I) monohydrate appeared as colorless solid, mp 297–300 °C. Anal. Calcd for $C_{24}H_{22}NOP_2S_2Na$: C, 58.89; H, 4.53; N, 2.86; S, 13.09; P, 12.66. Found: C, 58.84; H, 4.28; N, 3.00; S, 13.19; P, 12.65.

Bis(imidotetraphenyldithiodiphosphinato-*S*,*S*′)iron(II) appeared as pale green crystals, mp 285–286 °C. Anal. Calcd for $C_{48}H_{40}N_2P_4S_4Fe$: C, 60.50; H, 4.23; N, 2.94; S, 13.46; P, 13.00; Fe, 5.86. Found: C, 60.23; H, 4.06; N, 3.04; S, 13.57; P, 12.96; Fe, 5.85.

Bis(imidotetraphenyldithiodiphosphinato-*S*,*S*′)cobalt(II) appeared as green crystals, mp 305–308 °C. Anal. Calcd for $C_{48}H_{40}N_2P_4S_4Co$: C, 60.31; H, 4.22; N, 2.93; S, 13.42; P, 12.96; Co, 6.17. Found: C, 59.05; H, 4.36; N, 3.09; S, 13.50; P, 13.07; Co, 6.05.

Bis(imidotetraphenyldithiodiphosphinato-*S*,*S*′)copper(II) appeared as a dark violet solid, mp 172–174 °C. Anal. Calcd for $C_{48}H_{40}N_2P_4S_4Cu$: C, 60.02; H, 4.20; N, 2.92; Cu, 6.61. Found: C, 59.96; H, 4.53; N, 2.80; Cu, 7.06.

Tris(imidotetraphenyldithiodiphosphinato-*S*,*S*′)tricopper(I) appeared as pink crystals, mp 223–224 °C. Anal. Calcd for $C_{72}H_{60}N_3P_6S_6Cu$: C, 56.30; H, 3.94; N, 2.74; Cu, 12.41; mol wt, 1536. Found: C, 56.76; H, 4.07; N, 2.68; Cu, 12.63; mol wt (benzene), 1566.

Tris(imidotetraphenyldithiodiphosphinato-*S*,*S*′)tricopper(I) carbon tetrachloride solvate appeared as pale pink crystals, mp 116–118 °C. Anal. Calcd for $C_{72}H_{60}N_3P_6S_6Cu_3 \cdot 2^1/_2CCl_4$: C, 46.57; H, 3.15; N, 2.19; Cu, 9.92; mol wt, 1921. Found: C, 45.81; H, 2.77; N, 2.32; Cu, 10.15; mol wt (benzene), 1917.

Tris(imidotetraphenyldithiodiphosphinato-*S*,*S*′)tetracopper(I) dichlorocuprate(I) carbon tetrachloride solvate appeared as pink crystals, dec pt ~228 °C. Anal. Calcd for $[Cu_4(C_{24}H_{20}NP_2S_2)_3][CuCl_2]CCl_4$: C, 46.44; H, 3.20; N, 2.23; S, 10.19; Cu, 16.83; mol wt, 1888. Found: C, 47.30; H, 3.20; N, 2.21; S, 10.06; Cu, 16.39; mol wt (benzene), 1800.

Tris(imidotetraphenyldithiodiphosphinato-*S*,*S*′)tetracopper(I) perchlorate appeared as colorless crystals, dec pt ~260 °C. Calcd for $[Cu_4(C_{24}H_{20}NP_2S_2)_3]ClO_4$: C, 50.90; H, 3.56; N, 2.47; Cu, 14.96. Found: C, 51.44; H, 3.73; N, 2.59; Cu, 14.74.

Bis(imidotetraphenylthioxodiphosphinato-*S*,*O*)copper(II) appeared as brown crystals, mp 146–148 °C. Anal. Calcd for $C_{48}H_{40}N_2P_4S_2O_2Cu$: C, 62.10; H, 4.34; N, 3.02; Cu, 6.84. Found: C, 62.03; H, 4.41; N, 3.00; Cu, 6.98.

Bis(imidotetraphenylthioxodiphosphinato-*S*,*O*)nickel(II) appeared as green crystals, mp 186–188 °C. Anal. Calcd for $C_{48}H_{40}N_2P_4S_2O_2Ni$: C, 62.42; H, 4.37; N, 3.03; N, 6.36. Found: C, 62.26; H, 4.48; N, 3.05; Ni, 6.17.

Bis(imidotetramethyldithiodiphosphinato-*S*,*S*′)cobalt(II) appeared as blue crystals, mp 202–204 °C. Anal. Calcd for $C_8H_{24}N_2P_4S_4Co$: C, 20.92; H, 5.27; N, 6.10; S, 27.92; P, 26.97; Co, 12.83. Found: C, 20.82; H, 5.02; N, 6.35; S, 28.17; P, 26.72; Co, 12.84.

Spectral Measurements. Raman spectra were recorded with a Jarrell-Ash 25-500 double Ebert monochromator using a water-cooled

(8) O. Siiman, M. Wrighton, and H. B. Gray, *J. Coord. Chem.*, **2**, 159 (1972).

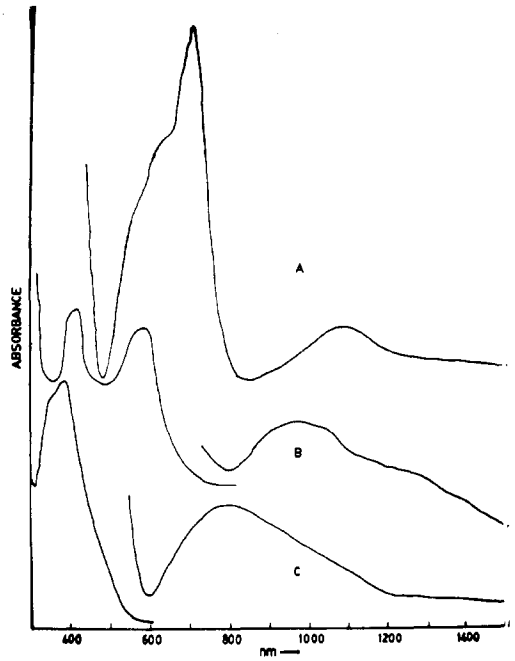

Figure 1. Electronic absorption spectra of (A) bis(imidotetraphenylthioxodiphosphinato-*S,O*)nickel(II) (1.0 mM in CH_2Cl_2), (B) bis(imidotetraphenyldithiodiphosphinato-*S,S*)copper(II) (Nujol mull), and (C) bis(imidotetraphenylthioxodiphosphinato-*S,O*)copper(II) (1.0 mM in $CHCl_3$).

Hammamatsu R500 photomultiplier tube for detection. Spectra-Physics Model 165 argon and krypton ion laser excitation was employed. Raman spectra of colorless or weakly absorbing solids were obtained by packing powdered samples into quartz capillary tubes. Incident laser light entered at ~45° to the capillary tube long axis. Single crystals were mounted such that their longest axis was parallel to the incident light beam. Spectra of colored samples were obtained with a rotating cylindrical stainless steel cell which had a circular groove packed with powdered material. Incident laser light impinged the packed groove at about a 45° angle. Scattered light was always collected at 90° to the incident beam. Spectral conditions are reported in the figure captions. Frequency readings were calibrated with emission lines of a neon spectral calibration lamp.

Infrared spectra were measured with a Perkin-Elmer Model 283 double beam grating instrument. Calibration of the instrument was performed with polystyrene film and water vapor. Electronic absorption spectra were recorded on a Cary 14 spectrophotometer.

Results and Discussion

Stereochemical Trends. In Figure 1 are shown the electronic absorption spectra of $Ni^{II}L'_2$, $Cu^{II}L'_2$, and $Cu^{II}L_2$ between 300 and 1500 nm. The green nickel(II) complex shows band maxima at 9260 and 14 390 cm^{-1}, with several weaker shoulders at 15 870 and 17 390 cm^{-1}. In accord with previous assignments[2a] of similar bands in $Ni^{II}L_2$ and $Ni^{II}L''_2$ the above two-band systems are assigned to spin-allowed ligand field transitions, $\nu_2(^3T_1(F) \rightarrow {}^3A_2(F))$ and $\nu_3(^3T_1(F) \rightarrow {}^3T_1(P))$, respectively, if a tetrahedral Ni(II) core is assumed. For the purposes of a Tanabe-Sugano analysis[9] the midpoint of the higher energy band system is taken at 15 500 cm^{-1}. Estimated ligand field parameters, $10Dq = -4875$ cm^{-1} for $B = 750$ cm^{-1}, $C = 3315$ cm^{-1}, gave calculated excited-state energies, 9225 and 15 375 cm^{-1}. The lowest energy ligand field band $\nu_1(^3T_1(F) \rightarrow {}^3T_2(F))$ was not observed but would be expected in the infrared at about $|10Dq| = 0.5$ μm^{-1}. For T_d $Ni^{II}S_4$ cores $|10Dq|$ was estimated to fall in the 4000–4500-cm^{-1} range. The slightly larger $|10Dq|$ value for T_d $Ni^{II}S_2O_2$ is not consistent with an opposite trend for the tetrahedral Co(II) complexes,[2a] $Co^{II}L_2$ ($10Dq = -4027$ cm^{-1}) and $(((C_6H_5)_2PO)N)_2Co^{II}$ ($10Dq = -3959$ cm^{-1}). $Co^{II}S_4$ absorption bands though are observed at lower energy than the corresponding ones of $Co^{II}O_4$. The electronic spectra of $Cu^{II}L'_2$ and $Cu^{II}L_2$ both show only one predominant band in the near-infrared region at 12 500 and 10 260 cm^{-1}. Previously reported near-infrared bands[2e] for $Cu^{II}L_2$ were at 10 870 cm^{-1} ($\epsilon = 400$) and 7250 cm^{-1} (very weak). Our mull spectrum of $Cu^{II}L_2$ showed only one major band similar to the spectrum of $Cu^{II}L'_2$. No further electronic absorption bands for either Cu(II) complex are observed at lower energies in the near-infrared or infrared. The intensity and location of these bands are in agreement with the characteristics of four-coordinate Cu(II) ligand field spectra. Up to four d–d transitions are possible for d^9 Cu(II) chromophores; however, high symmetry of donor atom environments usually limits the actual spectra to the appearance of only one or two ligand field bands.[10] Since the lowest energy band for the square-planar $Cu^{II}O_4$ complex, $(((C_6H_5)_2PO)N)_2Cu^{II}$, has been reported[4] at 14 000 cm^{-1}, a comparison shows the order $Cu^{II}O_4 > Cu^{II}O_2S_2 > Cu^{II}S_4$ for this band with imidodiphosphinate ligands. A regular downward trend in steps of 1500 and 2240 cm^{-1} upon sulfur-for-oxygen substitution is regarded by us to reflect both a small distortion toward tetrahedral geometry in the sulfur compounds and a characteristic of sulfur–ligand binding. The ligand field strengths of other ligands and metals in a specific geometry usually follow the same trend, $MO_4 > MO_2S_2 > MS_4$. More intense absorption bands in the near-ultraviolet region at 25 640 cm^{-1} in $Cu^{II}L'_2$ and 23 800 and 17 090 cm^{-1} in $Cu^{II}L_2$ are undoubtedly of charge-transfer origin and are discussed (vide infra) in connection with resonance Raman spectra.

Interpretations of electron paramagnetic resonance spectra that are now available for the $Cu^{II}O_4$, $Cu^{II}O_2S_2$, and $Cu^{II}S_4$ imidodiphosphinate complexes support the above conclusions. A polycrystalline sample of the $Cu^{II}O_4$ complex was shown[4] to present a two g value spectrum, $g_{\parallel} = 2.35$, $g_{\perp} = 2.08$, $|A_{\parallel}| = 156.3 \times 10^{-4}$ cm^{-1}, and $|A_{\perp}| = 9.7 \times 10^{-4}$ cm^{-1}, that is characteristic of square-planar copper–oxygen atom environments[11] such as in Cu^{II}(EDTA), $g_{\parallel} = 2.337$, $g_{\perp} = 2.090$, and $|A_{\parallel}| = 160 \times 10^{-4}$ cm^{-1}, and Cu^{II}(citrate), $g_{\parallel} = 2.349$, $g_{\perp} = 2.074$, and $|A_{\parallel}| = 150 \times 10^{-4}$ cm^{-1}. Reported spectra[2e] of $Cu^{II}L_2$ in CH_2Cl_2 yield a very narrow signal, $g_{\parallel} = 2.107$, $g_{\perp} = 2.030$, $|A_{\parallel}| = 119 \times 10^{-4}$ cm^{-1}, and $|A_{\perp}| = 19 \times 10^{-4}$ cm^{-1}. When this was compared[12] with EPR data of other planar and tetrahedral $Cu^{II}S_4$ cores, it placed $Cu^{II}L_2$ results in an intermediate geometrical category. Our own initial EPR spectra of $Cu^{II}L'_2$ (polycrystalline sample) show $g_{\parallel} = 2.18$, $g_{\perp} = 2.02$, and $|A_{\parallel}| = 176 \times 10^{-4}$ cm^{-1}. These parameters are more consistent with spectra reported for $Cu^{II}O_2S_2$ square-planar environments in $Cu(SPhCCHCPhO)_2$[13] (polycrystalline), $g_{\parallel} = 2.136$, $g_{\perp} = 2.026$, $|A_{\parallel}| = 181.6 \times 10^{-4}$ cm^{-1}, and $|A_{\perp}| = 36.5 \times 10^{-4}$ cm^{-1}, and $Cu(SCH_3CHCCH_3O)_2$[14] (*o*-terphenyl solution at 77 K), $g_{\parallel} = 2.132$ and $|A_{\parallel}| = 184.5 \times 10^{-4}$ cm^{-1}.

In the series of first-row transition-metal complexes with imidodiphosphinates, only for donor atoms X = S and Y = S does a consistent tetrahedral $M^{II}S_4$ core geometry emerge for M = Mn, Fe, Co, Ni, and Cu. Present evidence in the Cu(II) case suggests a distorted geometry closer to square planar than tetrahedral. The tetrahedral trend is broken for $M^{II}O_2S_2$ complexes in going from Ni(II) to Cu(II) and for $M^{II}O_4$ complexes in going from Co(II) to Ni(II). $((C_6H_5)_2PO)_2Ni^{II}$ appears[2a] to be associated in an oligomeric form. The key structure-determining factor appears to be the introduction of sulfur atoms and not the chelate ring geometry. In both

(9) Y. Tanabe and S. Sugano, *J. Phys. Soc. Jpn.*, **9**, 753, 766 (1954).

(10) (a) J. Ferguson, *J. Chem. Phys.*, **40**, 3406 (1964); (b) R. D. Willet, O. L. Liles, Jr., and C. Michelson, *Inorg. Chem.*, **6**, 1885 (1967).
(11) B. G. Malmstrom and T. Vanngard, *J. Mol. Biol.*, **2**, 118 (1960).
(12) U. Sakaguchi and A. W. Addison, *J. Am. Chem. Soc.*, **99**, 5189 (1977).
(13) D. Rehorek, R. Kirmse, and P. Thomas, *Z. Anorg. Allg. Chem.*, **385**, 297 (1971).

$Mn^{II}L_2$ and $Cu^{I}_4L_3^+$ crystal structures,[2d,5] the ligand S···S bite distances averaged 4.02 (4) Å. Similarly, $Ni^{II}L''_2$ and $Fe^{II}L''_2$ showed bite distances[2c] of 3.79 (12) Å. Comparison of PS bond distances (averaging 2.03 Å) against PO bond distance (~1.50 Å) shows that the replacement of sulfur by a smaller atom, oxygen, will decrease the donor atom bite distance in L'. The O,S ligand can more readily accommodate the ~90° XMY angles needed for square-planar MO_2S_2 geometry. Large bite distances for dithioimidodiphosphinates in contrast to distances in other bidentate sulfur ligands[15] were thought to arise from steric repulsions between phenyl or methyl groups attached to different P atoms of the same ligand. Structures show that steric interactions only force open the flexible PNP angle when the chelate ring assumes a nearly planar geometry or when axial–axial methyl group configurations are present.

Tris octahedral complexes, $Fe^{III}L_3$ or $Co^{III}L_3$, were not stabilized but an $Fe^{III}L'_3$ complex (high-spin d^5 Fe(III) ion) was isolated.[16] $Ni^{II}L_2$ was reported[2a] capable of increasing its coordination number beyond 4 by 1:1 and 2:1 pyridine–$Ni^{II}L_2$ adduct formation. Bromination of $Fe^{II}L_2$ in dichloromethane gave pale red crystals of a compound analyzed as a 1:1:1 ratio of Fe:L:Br. In addition, diamagnetic $Pd^{II}L_2$ and $Pt^{II}L_2$ chelates required to contain square-planar $M^{II}S_4$ cores were reported.[2a] Long M–S bond distances with M = Pt or Pd can accommodate a square-planar geometry for bis(dithioimidodiphosphinates). We predict that tris complexes of larger second- and third-row transition-metal ions will be stable.

Oxidation–Reduction Behavior and Structure–Reactivity Correlations. Unlike the autoxidation[17] that generally occurs with carbon–sulfur containing thiolate ligands (even in dithioureidodiphenylthiophosphinates,[17c] where one of the PS groups of L is changed to CS), dithioimidodiphosphinates form stable bis chelates in the presence of metal ions Mn^{II}, Fe^{II}, and Co^{II} which have easily accessible higher oxidation states. Typically, other thiophosphinic acids[6b] are oxidized to form dimeric disulfides in the same way as CS thiols. No evidence for this behavior for L (or L'' and L') was found. The presence of a thiol isomer of HL which was rigorously excluded from IR spectral data (vide infra) may be a requirement for disulfide formation. Facile dimerization of ionized thiols under basic conditions shows that thiolates are just as susceptible to oxidation. Dilute solutions of NaL show no tendency to yield L dimers. In fact, dropwise addition of aqueous NaL solution to ferric salt solutions leads to reduction of Fe^{III} to Fe^{II} and oxidation of the ligand L to HL', the monooxo-substituted derivative. Since methylation of L at a sulfur position was demonstrated,[1a] P=S bonds of L seem to have no unique property that would prevent S–S dimer formation. Phosphorus–sulfur compounds such as P_4S_9 and P_4S_{10} form adamantane-like cage structures[18] and oxidation of some thiols (dithioacetylacetone) proceeds to produce thioether dimers[7a-c] with the same basic cage structure. No evidence of L dimerization of this type is observed. Probably the five-coordination that is required of P atoms is not compatible with other structures which have contained four-coordinate C atoms, four-coordinate P atoms, three-coordinate P atoms, and three-coordinate Cu^I atoms.[5]

The cupric–dithioimidodiphosphinate reaction is analogous to the ferric–thiolate one in two respects. Reduced metal, Cu^I, and oxidized ligand, HL', are formed; however, no monomeric Cu^IL neutral complex has been isolated. Rather, several cluster complexes, Cu_3L_4, $Cu^I_3L_3$, $Cu^I_3L_3 \cdot 2^1/_2CCl_4$, $Cu^I_4L_3^+ \cdot Cu^ICl_2^- CCl_4$, and $Cu^I_4L_3^+ClO_4^-$, were prepared. The tri- and tetranuclear Cu^I complexes of L can be related to the second of three classes of copper–sulfur ligand clusters that contain copper exclusively in its lower valent state: (class 1) $Cu^I_8S_{12}$ core, an 8 Cu^I cube, and 12 S icosahedron, with dithiolate,[15c] D-pencillamine,[6a] and β,β-dimethylcysteamine;[19] (class 2) $Cu^I_4S_6$ core, a 4 Cu^I tetrahedron and 6 S octahedron (adamantane-like cage), with benzenethiolate[20] and thiourea;[21] (class 3) $Cu^I_4S_6$ core, a 4 Cu^I tetrahedron and two 4 S tetrahedra, with diethyldithiocarbamate.[22] The predictions of valence bond theory are realized in structure–bonding relations of Cu^I and its compounds. Linear two-coordinate (sp hybridized), trigonal-planar three-coordinate (sp^2), and tetrahedral four-coordinate (sp^3) Cu are acceptable structures wherein 4s, 4p bonding orbitals are used as electron pair acceptor orbitals for ligand donor atom electron pairs. Since Cu^I–S bond distances ~2.2–2.3 Å would give an intramolecular S···S distance of ~4.5 Å and S···S bite distances are ≤4 Å for L a linear 1:1 Cu^I:L complex is not expected to form. Preferred oligomeric forms, $[CuL]_n$, are dictated by ligand geometry and limitations on Cu^I stereochemistry. An obvious $n = 2$ structure

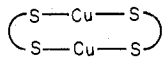

with linear Cu^IS_2 geometry, suffers from the instability of long Cu···Cu contact forced by an S···S bite distance of ~4 Å. A more acceptable structure, with trigonal-planar Cu^IS_3 geometry

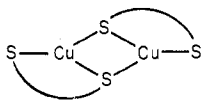

causes very small angles (60–70°) about S due to required trigonal SCuS angles. Solutions of $Cu^{II}L_2$ were unstable. Neutral Cu_3L_4 and Cu_3L_3 compounds were prepared but were not as stable to redox activity as the cationic $Cu_4L_3^+$ clusters. $Cu^I_3L_3$ solutions were converted by Cu(II) salts from colorless to dark violet ones containing a sulfur-coordinated Cu^{II} center and hence $Cu^I_3L_4^+X^-$ crystals. $Cu^I_4L_3^+$ clusters show no further reaction in the presence of Cu^{II} salt. Cu_3L_3 is also oxidizable with Fe^{III} salt, I_2, and NaL and H_2O_2 solutions. From known kinetic data and their associations with d-orbital metal ion configurations both Cu^I, d^{10} and Cu^{II}, d^9 complexes are expected to be labile to substitution reactions. The Cu^I clusters, however, appear to be less labile, possibly being further stabilized by nonbonded Cu···Cu (2.7–2.8 Å) and, to a much lesser extent, interchelate ring nonbonded S···S (3.8–3.9 Å) interactions. The difference in reactivity of $Cu^I_3L_3$ and $Cu^I_4L_3^+$ can be rationalized by fewer Cu···Cu contacts in the former and by the sulfur atom environments. In $Cu^I_4L_3^+$ all S atoms show a tetrahedral arrangement of one P and two Cu^I atoms and one lone pair of electrons to produce a trigonal-pyramidal geometry about each S atom. In $Cu^I_3L_3$ the deficiency of Cu atoms precludes the same arrangement about every S atom. Some two-coordinate S environments are ex-

(14) O. Siiman, unpublished results.
(15) (a) R. Beckett and B. F. Hoskins, *Chem. Commun.*, 909 (1967); (b) C. J. Fritchie, *Acta Crystallogr.*, **20**, 107 (1966); (c) F. J. Hollander and D. Coucouvanis, *J. Am. Chem. Soc.*, **96**, 5646 (1974).
(16) J. Rawlings, O. Siiman, and H. B. Gray, *Proc. Natl. Acad. Sci. U.S.A.*, **71**, 125 (1974).
(17) (a) K. Knauer, P. Hemmerich, and J. D. vanVoorst, *Angew. Chem., Int. Ed. Engl.*, **6**, 262 (1967); (b) D. H. Gerlach and R. H. Holm. *Inorg. Chem.*, **8**, 2292 (1969); (c) H. Groeger and A. Schmidpeter, *Chem. Ber.*, **100**, 3216 (1967).
(18) A. F. Wells, "Structural Inorganic Chemistry", 4th ed., Oxford University Press, London, 1976, p 694.
(19) H. J. Schugar, C. Ou, J. A. Potenza, R. A. Lalancette, and W. Furey, Jr., *J. Am. Chem. Soc.*, **98**, 3047 (1976).
(20) I. G. Dance and J. C. Calabrese, *Inorg. Chim. Acta*, **19**, L41 (1976).
(21) E. H. Griffith, G. W. Hunt, and E. L. Amma, *J. Chem. Soc., Chem. Commun.*, 432 (1976).
(22) R. Hesse, *Ark. Kemi*, **20**, 481 (1963).

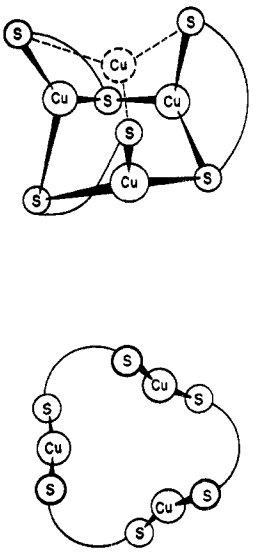

Figure 2. Suggested structures for $Cu^{I}_{3}L_{3}$.

pected. In previous studies[23] of the structure and stability of cuprous complexes with sulfur-containing ligands, several rules for Cu^{II} sulfur complexation were proposed. The third rule (cuprous mercaptides, with more than one two-coordinated sulfur atom per metal center, are unstable) can be used as a guide for probable $Cu^{I}_{3}L_{3}$ structures. Insofar as possible three-coordinate sulfur atom sites are maintained. Removal of the unique Cu^{I} atom located on a threefold symmetry axis of $Cu^{I}_{4}L_{3}^{+}$, shown in Figure 2, would leave a structure with a $Cu^{I}_{3}S_{3}$ ring, three two-coordinate sulfur atoms, and three three-coordinate sulfur atoms. An alternative geometry in which all three axial Cu–S bonds pictured in Figure 2 are located in equatorial positions with respect to the ring may be the favored one. Addtion of L to $Cu^{I}_{3}L_{3}$ is unlikely to maintain a $Cu_{3}S_{3}$ ring structure in which Cu···Cu distances are in the 2.7–2.8 Å range. Since the ligand bite distance of 4.0 Å does not match, coordination of both sulfur atoms of each ligand in $Cu_{3}L_{4}$ (as shown by IR spectra) would not be possible by simple cis addition across one of the Cu···Cu pairs. An open ring structure for $Cu^{I}_{3}L_{3}$, also shown in Figure 2, is similar to the one described by Dance[24] for a $Cu_{5}S_{6}$ cluster. Only the Cu^{I} atoms that lie above and below the central Cu^{I} triangle are missing. The existence of more than one two-coordinate S atom per metal atom is predicted to give an unstable open ring structure. Breakup of the ring structure appears necessary to formation of a $Cu_{3}L_{4}$ cluster.

Qualitative Assignment of Vibrational Modes. Infrared spectra between 300 and 1800 cm^{-1} for the tetraphenyldithioimidodiphosphinate (L) derivatives, HL, $Mn^{II}L_{2}$, $[Cu^{I}_{4}L_{3}^{+}][Cu^{I}Cl_{2}^{-}]CCl_{4}$, $[Cu^{I}_{4}L_{3}^{+}][ClO_{4}^{-}]$, $Cu^{I}_{3}L_{3}$, and $Cu^{I}_{3}L_{3}\cdot 2^{1}/_{2}CCl_{4}$ in Figure 3, and for derivatives, NaL, $[Cu^{II}(NH_{3})_{4}^{2+}][L^{-}]_{2}$, and $Cu^{II}L_{2}$, as well as the tetraphenylthioxoimidodiphosphinate (L′), $Cu^{II}L'_{2}$ in Figure 4. The Raman spectra (with the exception of $[Cu^{II}(NH_{3})_{4}^{2+}][L^{-}]_{2}$) are displayed in Figures 5 and 6. Infrared spectra of the tetramethyldithioimidodiphosphinates (L″), HL″, and $Co^{II}L''$ and the Raman spectrum of HL″ are shown in Figure 7.

Tentative vibrational mode assignments[1a] for the infrared bands of HL, KL, and some other ligand derivatives have been made before by Schmidpeter et al. Infrared bands of principal interest[1b] in HL′ and its derivatives were also assigned. With our acquisition of Raman spectral data and the ensuing normal mode analysis, it became obvious that several modifications

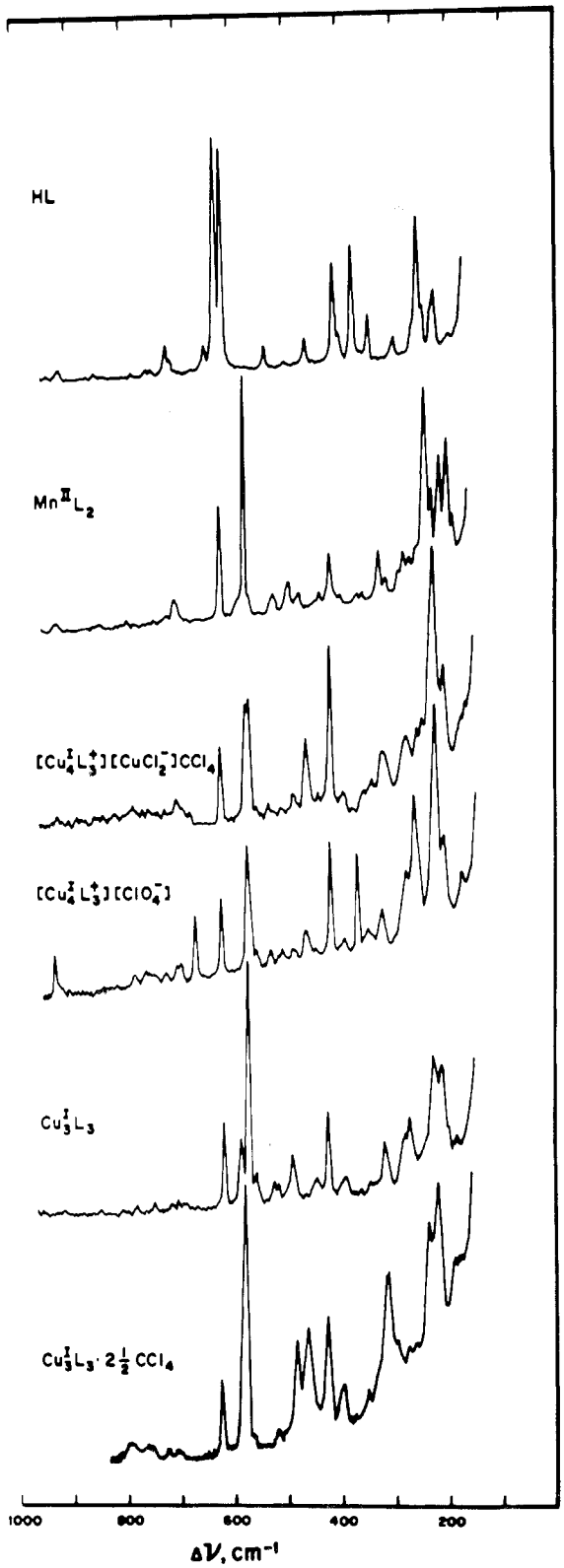

Figure 5. Raman spectra, solid or crystal. Experimental conditions (top to bottom) (scan rate, 0.5 cm^{-1}/s; excitation, 647.1 nm Kr^{+}): power 200 mW, slit width 5.0 cm^{-1}, sensitivity 8200 counts/s, time constant 2 s; 200, 5.0, 4700, 2; 270, 5.0, 4500, 2; 120, 5.0, 3000, 2; 200, 5.0, 4000, 2; 150, 7.0, 4000, 5.

in the preliminary vibrational assignments of Schmidpeter et al. were to be made.

Spectral differences in HL and deprotonated ligand, L^{-}, of alkali metal salts or metal chelates are marked for PNP and PS vibrations as well as for the presence (or lack thereof) of

(23) V. Vortisch, P. Kroneck, and P. Hemmerich, *J. Am. Chem. Soc.* **98**, 2821 (1976).
(24) I. G. Dance, *J. Chem. Soc., Chem. Commun.*, 68 (1976).

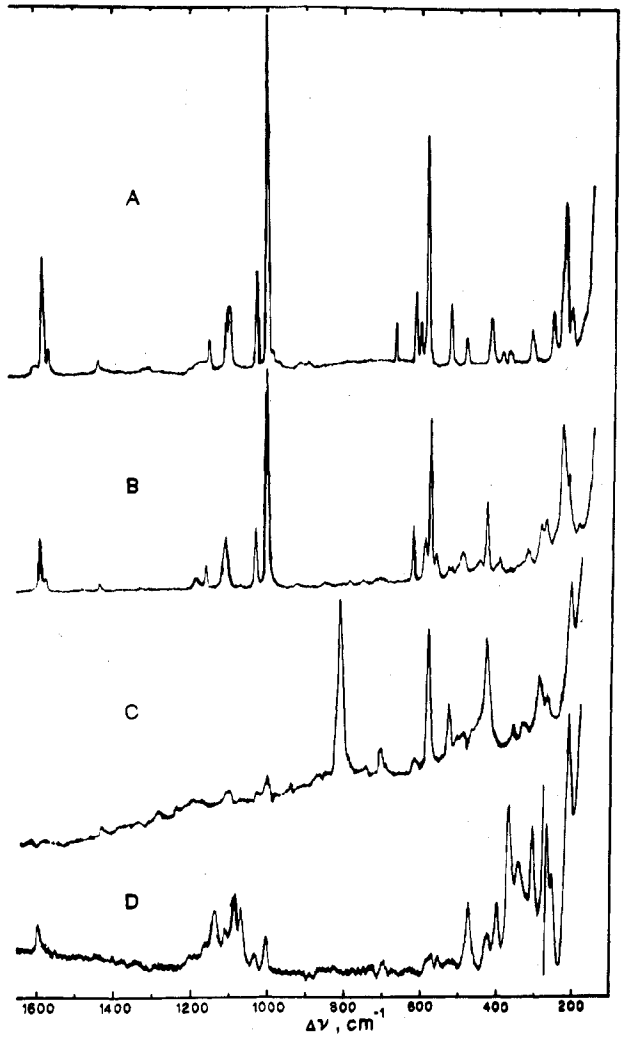

Figure 6. Raman spectra of A, NaL (solid), B, $Cu^{I}_{3}L_{3}$ (crystal), C, $Cu^{II}L_{2}$ (solid), and D, $Cu^{II}L'_{2}$ (solid). Experimental conditions (scan rate, 0.5 cm^{-1}/s): A, excitation 647.1 nm, Kr^{+}, power 120 mW, slit width 5.7 cm^{-1}, sensitivity 2000 counts/s, time constant 2 s; B, 647.1, Kr^{+}, 150, 5.0, 4800, 2; C, 647.1, Kr^{+}, 200, 10.0, 1000, 5; D, 488.0, Ar^{+}, 300, 8.7, 2000, 5.

NH group vibrations. HL shows bands due to ν(N–H) at 2620 cm^{-1} and δ(N–H) at 1324 cm^{-1}. The deuterated ligand, formed by titration of NaL in D_2O with DCl in D_2O to precipitate the water insoluble DL, showed new infrared bands at 2278 (mw), 2105 (w), 1070 (vs), and 825 (ms) cm^{-1}. The band at 2278 cm^{-1} is associated with ν(C–D) from deuterated phenyl groups (with a diatomic harmonic oscillator model ν(C–D) is predicted at 2245 cm^{-1} for ν(C–H) at 3058 cm^{-1} in HL). The weak 2105-cm^{-1} band is therefore assigned to ν(N–D) even though the latter is calculated to appear at 1913 cm^{-1} by the diatomic model. Changes in the coupling of ν(N–H) and ν(N–D) to other ligand vibrations may explain the ~200-cm^{-1} discrepancy with the calculated isotopic shift. The strong band at 1070 cm^{-1} is assigned to partially deuterated phenyl group C–D bending vibrations, and a medium strong band at 825 cm^{-1} may originate from δ(N–D).

ν_{as}(P–N–P) occurs in HL as a very strong IR band at 920 cm^{-1} and increases by about 300 cm^{-1}, when the NH proton is removed, to reflect the increased PN bond order. A broad, very strong IR band in the 1170–1230-cm^{-1} region is assigned to ν_{as}(P···N···P). The symmetric P···N···P (bent structure) stretching vibration should be IR active and ν_{as}(PNP) should be Raman active but neither band has been observed in the respective IR or Raman spectra of any imidodiphosphinate.

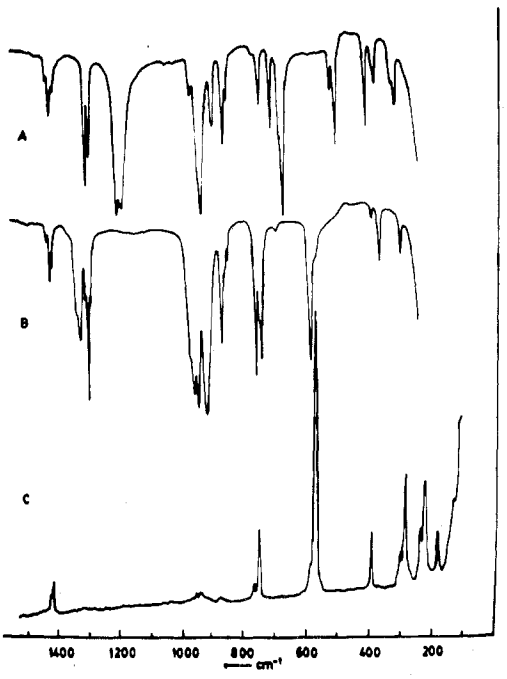

Figure 7. Infrared spectra of HL″ and $Co^{II}L''$ (KBr pellets) and Raman spectra of solid HL″. Experimental conditions: excitation 647.1 nm Kr^{+}; power 65 mW; slit width 5.5 cm^{-1}; sensitivity 3000 counts/s; time constant 5 s; scan rate 0.5 cm^{-1}/s.

No regular Raman band assignable to ν_{s}(P···N···P) was observed either. Only in the resonance Raman spectrum of $Cu^{II}L_{2}$ was ν_{s}(P···N···P) located at 813 cm^{-1}. Its location in the 800 cm^{-1} vicinity was substantiated by normal-mode calculations.[25] On the basis of the frequency difference, ν_{as}(PNP) – ν_{s}(PNP) = 1175 – 813 = 362 cm^{-1} in $Cu^{II}L_{2}$, we would expect ν_{s}(P–N–P) in HL to appear in the region 558 (=920 – 362) cm^{-1}. A weak, broad infrared band at 572 cm^{-1} was previously assigned to ν_{s}(P–N–P) in HL. Since only an extremely weak feature was detected near 570 cm^{-1} in the Raman spectrum of HL, the location of ν_{s}(P–N–P) remains undetermined at present.

The unsymmetrical ligand, HL′, shows a medium–weak IR band at 2695 cm^{-1} and a medium band at 1370 cm^{-1}, which are not present in the deprotonated $Cu^{II}L'_{2}$ complex. By analogy to HL, we assign these bands to NH stretching and bending modes. Therefore, HL′ is protonated in the same way at N as HL although O, being more electronegative than N, might preferably bind H. π-Bonding capabilities of P=O vs. P=N may favor the former bond.

Infrared bands, ν_{as}(P–N–P) of HL′ at 937 cm^{-1} and ν_{as}(P···N···P) of $Cu^{II}L'_{2}$ at 1200 cm^{-1}, are very similar in intensity, bandwidth, and position to the corresponding vibrational bands of HL and its deprotonated derivatives. Since L′ as a bidentate ligand has different donor atoms, O and S, widely apart in electronegativity, the two P···N bonds of chelate rings in $Cu^{II}L'_{2}$ would not be expected to have the same bond distance nor therefore bond order. The ligand asymmetry is expected to affect the intensity of ν_{s}(P···N···P) in the IR and Raman spectra. Since ν_{as}(PNP) for $Cu^{II}L'_{2}$ and $Cu^{II}L_{2}$ are found at about the same frequencies, ν_{s}(PNP) for the two complexes is also expected to be similar, i.e., at ~813 cm^{-1}. No band assignable to ν_{s}(PNP), however, was observed in the IR or Raman spectra of $Cu^{II}L'_{2}$.

Previous assignment[1b] of ν(P=S) in HL′ was made for a very strong IR band at 725 cm^{-1}. We prefer to assign a medium doublet at 635, 625 cm^{-1} to ν(P=S). This band does

(25) O. Siiman, to be submitted for publication.

Table I. Vibrational Frequencies (cm^{-1}) of Phosphorus-Neighboring Atom Stretching Modes[a]

		ν_{as}(PN)	ν_s(PN)	ν(PC)	ν_{as}(PS)	ν_s(PS)	ν(PO)
$Mn^{II}L_2$	IR	1218 vs, br		715 m, 700 vs, 692 sh	568 vs	585 mw	
	R			718 mw, 705 w, . . .	567 w, sh	580 s	
$Cu^{II}L_2$	IR	1175 vs, br		715 m, 700 vs, 688 w	563 vs	590 vw	
	RR		813 vs	. . ., 705 w, 690 vw		580 s	
$[Cu^{I}_4L_3^+][Cu^{I}Cl_2^-]CCl_4$	IR	1216 vs, 1225 sh		718 m, . . ., 692 vs	551 vs	570 vw, sh	
	R			. . ., 700 vw, . . .		570, 575 s	
$[Cu^{I}_4L_3^+][ClO_4^-]$	IR	1216 vs, br		718 m, . . ., 692 vs	551 vs		
	R			. . ., 700 vw, . . .		573 s	
$Cu^{I}_3L_3$	IR	1225 vs, 1210 sh		715 mw, . . ., 697 vs	558 vs	583 mw	
	R			720 vw, 705 vw, . . .	560 w	576 s, 590 w	
$Cu^{I}_3L_3 \cdot 2\frac{1}{2}CCl_4$	IR	1210 vs, br		715 mw, . . ., 697 vs	558 vs	580 mw	
	R			720 vw, 705 vw, . . .		581 s	
HL	IR	926, 920 vs, 935 s		720 s, 715 sh, 688 s	648 vs	610 mw	
	R			720 w, 713 vw, . . .	646 vw	616, 628 vs	
NaL	IR	1192, 1178 vs		710 s, 697 vs, 688 sh	602 s	577 s	
	R			. . ., . . ., . . .	602 w	575 s	
$[Cu(NH_3)_4^{2+}][L^-]_2$	IR	1213 vs, br		711 vs, 700 vs, 692 w, 688 mw	602 ms	578 ms	
$Cu^{II}L'_2$	IR	1200 vs, br		722 s, 698 vs, 690 vs	569 vs, 578 sh		1060 s, 1076 w
	R			. . ., 695 vw	570 vw		1062 m, 1079 m
HL′	IR	937 vs		722 vs, 710 sh, 690 vs	635, 625 m		1205, 1190 s
$Co^{II}L''_2$	IR	1198, 1187, 1180 vs		749 m, 713 m, 674 vs	505 m	521 m	
HL″	IR	912 vs		760 s, 739 ms, 742 sh, 690 w	584 s	570 vw, sh	
	R			765 vw, 739 m, . . ., . . .	585 vs, sh	570 vs	

[a] IR = infrared, R = Raman; RR = resonance Raman.

not appear in $Cu^{II}L'_2$ whereas strong IR bands at 722 cm^{-1} occur in both HL′ and $Cu^{II}L'_2$. In addition, $Cu^{II}L'_2$ shows a marked increase of IR-band intensity in the 540–570-cm^{-1} range. One strong band, at either 569 or 551 cm^{-1} (we prefer the latter since the sharp 569-cm^{-1} band resembles a sharp 554-cm^{-1} band in HL′), is assignable to ν(P···S) in $Cu^{II}L'_2$. Approximately a 70-cm^{-1} difference in ν(PS) for protonated vs. metal coordinated ligand then exists for both S,S and S,O imidodiphosphinate ligands. Compounds of L show two ν(PS) bands (vide infra).

Phosphorus–oxygen stretching vibrational bands are additions to the spectra of HL′ and $Cu^{II}L'_2$. ν(P=O) in HL′ was previously assigned[1b] to an IR band at 1202 cm^{-1}. Since HL shows no band in this region and $Cu^{II}L'_2$ exhibits an additional intense band and shoulder at 1060, 1076 cm^{-1} that was not present in HL′, we concur with this assignment. Both strong IR bands at 1205, 1190 cm^{-1} in HL′ and the two peaks at 1060, 1076 cm^{-1} in the copper complex are assigned to ν(PO). The P···O bond polarizability is expected to be large so that two medium Raman bands of $Cu^{II}L'_2$ at 1062, 1079 cm^{-1}, which are counterparts of IR bands, are assigned to ν(PO). No comparable Raman peaks were observed in spectra of L compounds in the 1050–1100-cm^{-1} region. An intense IR band and medium–weak Raman band are found for both L and L′ compounds between 1100 and 1130 cm^{-1}. This band is associated with phenyl group vibrations (vide infra). The doublet splitting of infrared and Raman bands is a feature common to PS and PO stretching modes in HL′ and $Cu^{II}L'_2$. Lack of strong Raman intensity in ν(P···S), which appeared as an intense band in Raman spectra of S,S ligand compounds, may arise from a lower PS bond order due to electron density withdrawal by the more electronegative O atom of the PO bond.

In previous assignments[1a] ν(P–C) was associated with strong IR bands near 1110 and 690 cm^{-1}. Our normal-coordinate calculations[25] show that P–C stretching modes are clustered together in a much smaller frequency range than 400 cm^{-1}. Several bands in the 725–680-cm^{-1} region of L and L′ compounds fit these predictions. Since weak Raman intensity appears in these bands and not bands between 730 and 800 cm^{-1} (linked to out-of-plane C–H vibrations of the phenyl groups), we prefer to associate the more polarizable P–C bonds with stretching vibrational bands from 725 to 680 cm^{-1} in the Raman spectra.

The CH_3 for C_6H_5 substituted ligand, HL″, shows IR bands at 2610 and 1314 cm^{-1}, which are assignable to ν(N–H) and δ(N–H) modes. Both bands are absent in the IR spectrum of deprotonated ligand in $Co^{II}L''_2$. As in compounds with L, broad, strong IR bands, ν_{as}(PNP), occur both in HL″ at 912 cm^{-1} and in $Co^{II}L''_2$ at 1190 cm^{-1}. No IR band near 1200 cm^{-1} is observed for HL″. Characteristic methyl group modes of vibration, $\delta(CH_3)$, $\rho(CH_3)$, and CH_3 wag, are assigned by reference to IR and Raman spectra[26] of tetramethyldiphosphine disulfide to bands that appear at 1410, 1290, 930, and 860 cm^{-1} in both HL″ and $Co^{II}L''_2$. A band assignable to ν_s(PNP) was not detected in either IR or Raman spectra of L″ compounds. Two new bands at 674, 684 (sh) and 505, 521 cm^{-1} in the IR spectrum of $Co^{II}L''_2$ are possible assignments for ν(P···S). Since L and L′ metal complexes showed a 70 cm^{-1} decrease in ν(PS) frequencies upon metal ion chelation, we assign the 505-, 521-cm^{-1} bands of $Co^{II}L''_2$ and strong 584-cm^{-1} IR band of HL″ to PS stretching modes. NaL″ also shows IR bands at 667 and 564 cm^{-1}. The relative intensity of the 667-cm^{-1} band is much lower in NaL″ than in $Co^{II}L''_2$. A much smaller frequency lowering of ν(PS) by 20 cm^{-1} relative to ν(PS) in HL″ concurs with the expected weaker Na···S interaction. Infrared bands near 670 cm^{-1} in $Co^{II}L''_2$ and NaL″ are then assigned to ν(P–C). Their appearance in L″ metal complexes and absence in HL″ might be attributed to a major structural difference between HL″ and $Co^{II}L''_2$ or NaL″. Since no hydrogen bonding interaction is present between sulfur atoms of HL″ to favor a cis isomer, HL″ probably adopts a trans PS bond conformation to minimize CH_3, CH_3 steric interactions and therefore possesses pseudo-inversion symmetry (of $PS(CH_3)_2$ groups) instead of the C_2 or C_s symmetry of MS_2P_2N chelate rings.

A summary of chelate ring and P–C bond stretching frequencies is given in Table I.

Phenyl Group IR and Raman Bands. Infrared band assignments for phenyl vibrations of some tetraphenyl-substituted compounds have already been summarized.[1a] A listing[27] of monosubstituted benzene ring normal modes and their Raman

(26) (a) A. H. Cowley and H. Steinfink, *Inorg. Chem.*, **4**, 1827 (1965); (b) M. Arshad, A. Beg, and S. H. Khawaja, *Spectrochim. Acta, Part A*, **24a**, 1031 (1968).

(27) F. R. Dollish, W. G. Fately, and F. F. Bentley, "Characteristic Raman Frequencies of Organic Compounds", Wiley-Interscience, New York, 1974, Chapter 13, p 170.

activity was also consulted. The nomenclature that was used in the latter discussions was adopted for band assignments herein. All examined tetraphenylimidodiphosphinates showed infrared bands invariant by position and relative band intensity at 1478 (w), 1435 (s) (ν(ring), derived from e_{1u} vibration of benzene), 1305 (w) (ν(ring), b_{2u}), 1290 (w) (δ_{CH}, a_{2g}), 1180 (w) (δ_{CH}, e_{2g}), 1160 (vw) (δ_{CH}, b_{2u}), 1108 (s) (ν(ring), a_{1g}, substituent sensitive), 1070 (w) (δ_{CH}, e_{1u}), 1028 (m) (δ_{CH}, e_{1u}), 998 (m) (δ(ring), b_{1u}), 970 (vw) (γ_{CH}, e_{2u}), 845 (w) (γ_{CH}, e_{1g}), and 618 cm^{-1} (δ(ring), e_{2g}). Unchanging phenyl group Raman bands and their corresponding assignments are found at 1438 (vw) (ν(ring), e_{1u}), 1185 (w, br) (δ_{CH}, e_{2g}), 1162 (w) (δ_{CH}, b_{2u}), 1108 (m) (ν(ring), a_{1g}), 1070 (vw) (δ_{CH}, e_{1u}), 1030 (δ_{CH}, e_{1u}), 1004 (vs) (δ(ring), b_{1u}), and 620 (mw) cm^{-1} (δ(ring), e_g). Infrared and Raman bands which are linked to the phenyl group in five other spectral regions and exhibited characteristic changes from one class of compound to another are listed with their most probable assignments in Table II. Undoubtedly, some of the bands that are observed in regions III, IV, and V are also assignable to skeletal bending modes of the ligand or chelate rings.

Phosphorus–Sulfur Modes and Structural Changes. Characteristic PS stretching modes (500–700 cm^{-1}) have been identified in the infrared[1a,28] and Raman spectra[29] of dithiophosphinates. Though dithioimidodiphosphinate ν(PS) bands were assigned previously, the S,S ligand gives rise to two ν(PS) bands, only one of which has been assigned with any certainty in the infrared region. The other ν(PS) mode is weak in the IR region and was first located in our Raman spectra. With reference to Table I divalent metal chelates, $M^{II}L_2$, M = Mn, Fe, Co, Cu, and Cu^I cluster compounds all show a lower frequency strong IR active ν(P⋯S) band a higher frequency intense Raman active ν(P⋯S) band. The order of ν(P⋯S) frequencies is $Cu^I_4L_3^+ < Cu^I_3L_3 < M^{II}L_2$. A parallel trend in the opposite direction is found in the approximate mutual exclusiveness of IR and Raman ν(PS) bands. A case for a structural and metal–sulfur bond strength relationship to ν(PS) can be made. The individual chelate rings in $Cu^I_4L_3^+$ are very nearly planar[5] so that the dihedral angle between the two PS bonds (viewed along the nonbonded P⋯P line) is about 0°. Both sulfur atoms of the ring are three-coordinate (bound to 2 Cu and 1 P atoms) and have a pyramidal structure. The above is not true of $M^{II}L_2$ structures (as in $Mn^{II}L_2$[2d]) wherein the dihedral PS angle is about 60° and S atoms are two-coordinate and have a bent geometry. Chelate ring M–S bond distances are significantly shorter (average 2.27 Å) for Cu^I–S than for Mn^{II}–S (average 2.45 Å) and P⋯S bond distances are longer, 2.053 Å, for $Cu^I_4L_3^+$ than, 2.013 Å, for $Mn^{II}L_2$. Point group symmetry C_s for CuS_2P_2N and C_2 for MnS_2P_2N, notwithstanding, flattening out of the chelate ring structure appears to reflect greater M–S bond strengths, lower PS bond strength, and in turn lower ν(PS) frequencies.

$Cu^I_3L_3$ cluster ν(PS) mode features appear to be intermediate to those of $Cu^I_4L_3^+$ clusters and $M^{II}L_2$ bis chelates. Removal of the uniquely positioned Cu atom of $Cu^I_4L_3^+$ provides a logical structural possibility for $Cu^I_3L_3$, illustrated in Figure 2. The most plausible alternative is a flattened-out structure obtained by converting all three axially located two-coordinate S atoms into equatorial positions of the chairlike Cu_3S_3 ring. The nonchelate ring aspect of the open ringlike structure shown in Figure 2 implies major geometric differences between $Cu^I_4L_3^+$ and $Cu^I_3L_3$. IR and Raman spectra do not give evidence of any major changes in structure. The intermediate character of ν(PS) band frequencies and relative IR and Raman intensities can be rationalized by an intermediate structure: three two-coordinate and three three-coordinate sulfur atom environments in the two postulated structures with one intact $Cu^I_3S_3$ ring.

With respect to intensity and position of ν(PS) modes in HL and HL″ a diametrically opposite relationship is observed. The higher frequency ν(P═S) is seen as a very strong band in the IR spectrum while the lower frequency ν(P═S) appears as a very strong band in the Raman spectrum. This trend is not strictly true for NaL and probably $[Cu(NH_3)_4^{2+}][L^-]_2$ wherein both ν(P⋯S) bands are about equally intense in the IR region. Only the lower frequency ν(P⋯S) band at 575 cm^{-1} is intense in the Raman spectrum. We suspect that these differences in ν(PS) mode characteristics for HL, HL″, and L^- are the result of substantial structural change. A structure for HL or HL″ wherein the two PR_2S halves of the molecule are related by pseudoinversion symmetry should exihibit the near mutual exclusiveness and switch in activity of IR and Raman ν_{as}(PS) and ν_s(PS) modes. In the ionized form of the ligand, L^-, the molecular structure is probably intermediate to that in the transition-metal chelates and the protonated ligand. Weak interaction between sodium and sulfur atoms allows the dihedral angle between PS bonds to open up beyond the ~60° angle in the $Mn^{II}L_2$ structure. The very intense lower frequency ν(PS) band in the Raman spectrum of NaL, similar to the one in the HL spectrum, is consistent with a structure for NaL that is more akin to the one for HL rather than $Mn^{II}L_2$.

Metal-Sensitive Vibrations. Low-temperature single-crystal electronic absorption spectra[2d] of $Mn^{II}L_2$ showed vibrational fine structure which contained progressions in quanta of the totally symmetric Mn–S stretching mode averaging 254 cm^{-1}. Since the associated excited states have the same electronic configuration as the $^6A_1$ ground state, we expect the ground state ν_{a_1}(Mn–S) model of $Mn^{II}L_2$ to have a frequency near 254 cm^{-1}. Since HL and NaL exhibit moderately strong Raman bands at 253 and 232 cm^{-1}, respectively, some confusion over the actual location of ν_{a_1}(Mn–S) in $Mn^{II}L_2$ is inherent. A single intense Raman band is observed at 242 cm^{-1} for $Mn^{II}L_2$. Substantially weaker interaction between Na(I) and ligand sulfur atoms is expected in NaL (a smaller downward shift of ν(PS) by 40 cm^{-1} instead of ~60 cm^{-1} in $Mn^{II}L_2$ is also observed) so that ν(Na⋯S) frequencies are anticipated below 200 cm^{-1}. The observation of bands in the 200–300-cm^{-1} region for NaL shows that ligand vibrational bands do interfere in the identification of ν(M–S) in this frequency range. Recording of the far-infrared spectra shown in Figure 8 of the metal chelates has however been very helpful. ν_{a_1}(Mn–S) should not be observed in the IR region for T_d $Mn^{II}S_4$ cores, but a band or bands originating from ν_{t_2}(Mn–S) will be both IR and Raman active. Spectra of both $Mn^{II}L_2$ and $Fe^{II}L_2$ show an intense Raman band near 245 cm^{-1} but no detectable band in the infrared at this location. Infrared bands at 275, 285 cm^{-1} have a counterpart in the Raman spectra of $M^{II}L_2$ complexes and are therefore assigned to ν_{t_2}(M^{II}–S). NaL and HL spectra do not show a similar relationship between identifiable IR and Raman bands between 200 and 300 cm^{-1}. Normal-mode calculations for tetrahedral MS_4 models support the assignment of ν_{t_2} to a higher frequency (by >20 cm^{-1}) vibrational band than ν_{a_1} (**F** and **G** matrix elements described before[30] were used).

For $Cu^I_4L_3^+$ and $Cu^I_3L_3$ clusters, an analysis of $\Gamma_{Cu\text{-}S}$ (the irreducible representations to which Cu–S stretching modes belong) in a symmetrical adamantane cage of composition Cu_4S_6 and T_d point symmetry gives ν(Cu–S) of species a_1 +

(28) R. G. Cavell, E. D. Day, W. Byers, and P. M. Watkins, *Inorg. Chem.*, **11**, 1759 (1972).
(29) S. Sunder, L. Hanlan, and H. J. Bernstein, *Inorg. Chem.*, **14**, 2012 (1975).
(30) K. Nakamoto, "Infrared and Raman Spectra of Inorganic and Coordination Compounds", 3rd ed., Wiley-Interscience, New York, 1978, p 432.

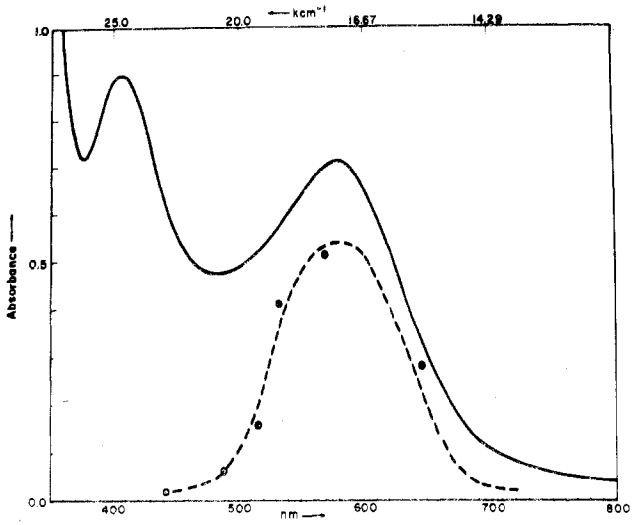

Figure 9. Electronic absorption and resonance Raman excitation spectra of Cu_3L_4 (solid).

$e + t_1 + 2\ t_2$, wherein a_1 and e modes are only Raman active, t_1 vibrations are neither Raman nor IR active, and t_2 vibrations are both Raman and IR active. Therefore, another qualitative approach was used to identify possible metal sensitive vibrational modes in the copper clusters. Below, are listed the ratio of P⋯S to M–S bonds and the intensity ratios of two Raman bands (generally located in the 400–500- and 200–250-cm^{-1} regions, respectively) relative to the symmetric P⋯S stretching band intensity.

	$Mn^{II}L_2$	$Na^{I}L$	$Cu^{I}_4L_3^+$	$Cu^{I}_3L_3$
P⋯S/M–S	1.0	1.0	2.0	1.5
$I_{420}/I(P\cdots S)$	0.3	0.3	0.8	0.6
$I_{220}/I(P\cdots S)$	1.4	1.1	2.0	1.7

The two identified Raman bands change relative intensity the most in metal complexes with L and are located in the metal–sulfur stretching frequency region. Due to symmetry considerations (different in each type of complex) the relative intensity of ν_s(M–S) is not expected to bear any exact relation to the number of M–S relative to P⋯S bonds. In addition, chelate ring structural changes might also be manifested in varying intensities of ν(M–S) Raman bands. Relative to NaL, $Mn^{II}L_2$ shows some increased intensity for the Raman band near 242 cm^{-1}, that was assigned to ν_{a_1}(Mn–S), but shows no change for the band at 425 cm^{-1}. Though structural variations are evident from ν(PS) modes for $Na^{I}L$ and $Mn^{II}L_2$, they affect Raman bands at 425 and 240 cm^{-1} minimally. The large relative increase in the intensity of the two Raman bands in this region for the $Cu^{I}_4L_3^+$ and $Cu^{I}_3L_3$ clusters is therefore attributed to a larger Cu–S contribution to these normal modes. Structural changes such as flattening out of the CuS_2P_2N ring and opening up of the PNP angle are not expected to be the major factors in determining Raman band intensities at ~420 and 220 cm^{-1}.

The resonance Raman spectrum of $Cu^{II}L_2$ shows bands at 825, 580, 425, 287, 213, and 530 cm^{-1} in order of relative intensity enhancement. Since little enhancement of phenyl ring (e.g., ~1000 cm^{-1}) or ν(P–C) vibrational bands was observed, electronic coupling between the metal chelate ring and phenyl ring is absent. The electronic absorption spectrum of Cu_3L_4 and the excitation profile obtained by plotting the relative intensity enhancement of the 820-cm^{-1} resonance Raman band against an internal standard, the ~1000-cm^{-1} phenyl group Raman band, are shown in Figure 9. Shown in Figure 1, $Cu^{II}L_2$ exhibits a very similar electronic absorption spectrum between 800 and 400 nm whereas $Cu^{II}L'_2$ shows no intense visible absorption band. Since two of the copper atoms in Cu_3L_4 are formally in the Cu(I) state, resonance Raman enhancement of the vibrations of only one chelate ring occurs. Therefore, a relative increase in normal Raman scattering (including phenyl group modes) in Cu_3L_4 was observed. The resonance Raman bands of $Cu^{II}L_2$ are, therefore, exclusively chelate ring vibrational bands; the highest frequency one is expected to be assignable to ν_s(P⋯N⋯P). In phosphonitrilic trimers[31] the ring breathing mode, $\nu_s(P_3N_3)$, was located at 785 cm^{-1} in $[Cl_2PN]_3$ and at 753 cm^{-1} in $[Ph_2PN]_3$. The most intense resonance Raman band at 825 cm^{-1} is assigned to ν_s(PNP). The next highest frequency band at 580 cm^{-1} and second most intense was observed in normal Raman spectra of other $M^{II}L_2$ compounds. It is assigned to ν_s(P⋯S). The third most intense resonance Raman band at 425 cm^{-1} might also be associated with the PNP linkage as the δ(PNP) mode, which should only be intense in the Raman region according to the observed intensities of IR and Raman bands of other symmetric chelate ring vibrations. A counterpart is detected in the normal Raman spectra of $M^{II}L_2$, $Cu^{I}_4L_3^+$, $Cu^{I}_3L_3$, and $Na^{I}L$. Some uncertainty remains as a weak infrared band occurs at 413 or 420 cm^{-1} for $Cu^{I}_4L_3^+$ and $Cu^{I}_3L_3$ clusters. The presence of $\delta_s(P_3N_3)$ at 671 cm^{-1} and $\delta_{as}(P_3N_3)$ at 336 cm^{-1} in phosphonitrilic trimers, though, makes δ(PNP) a logical assignment for the 425-cm^{-1} band in imidodiphosphinates. For $M^{II}L_2$ and $Na^{I}L$ no other Raman band in the 650–300-cm^{-1} region fits the requirement of very weak infrared band intensity. Some contribution from ν_{t_2}(Cu–S) which is both IR and Raman active for a tetrahedral Cu_4S_6 core structure would explain the presence of bands in both IR and Raman spectra of $Cu^{I}_4L_3^+$ (and $Cu^{I}_3L_3$) at ~425 cm^{-1}. For $Cu^{II}L_2$ both ν_{a_1}(Cu–S) and ν_{t_2}(Cu–S) are expected to be Raman active for a T_d $Cu^{II}S_4$ core. Accordingly, resonance Raman bands at 213 and 287 cm^{-1} are assigned to ν(Cu–S) by analogy to the assignment of Raman bands of $Mn^{II}L_2$ and other bis chelates. No Raman band is observed for $Na^{I}L$ in the 270–300-cm^{-1} range but $Cu^{I}_4L_3^+$ and $Cu^{I}_3L_3$ both exhibit a weak band(s) at ~275 cm^{-1}, which might be attributed to another Raman active ν_e(Cu–S) or ν_{t_2}(Cu–S) mode.

Acknowledgment. This work was supported, in part, by the Institute of General Medical Sciences, U.S. Public Health Service Grant GM-23072. J.V. also acknowledges support of the National Science Foundation through its Undergraduate Research Participation program.

Registry No. I, 65232-75-9; II, 65404-73-1; III, 73286-13-2; V, 65232-76-0; VI, 73274-77-8; VII, 73274-78-9; VIII, 61159-90-8; $Co^{II}L''_2$, 31747-72-5; $Fe^{II}L_2$, 31747-69-0; $Co^{II}L_2$, 31747-71-4; $Ni^{II}L'_2$, 73274-79-0; $Mn^{II}L_2$, 40362-04-7; HL, 6588-07-4; HL′, 17162-83-3; HL″, 18509-37-0; NaL, 73274-52-9; L^-, 16523-64-1.

Supplementary Material Available: Figure 3 (IR spectra), Figure 4 (IR spectra), Figure 8 (far-IR spectra), and Table II (vibrational frequencies of phenyl group modes) (5 pages). Ordering information is given in any current masthead page.

(31) A. C. Chapman and N. L. Paddock, *J. Chem. Soc.*, 635 (1962).